JETIR.ORG ISSN: 2349-5162 | ESTD Year : 2014 | Monthly Issue

JOURNAL OF EMERGING TECHNOLOGIES AND INNOVATIVE RESEARCH (JETIR)

An International Scholarly Open Access, Peer-reviewed, Refereed Journal

Unsteady MHD Casson Fluid Flow past a vertical plate through porous medium in presence of Soret-Dufour effect and radiation absorption with heat source/sink

[1]A.K. Shukla, [2]Aneesh Jayswal, [3]Mohammad Suleman Quraishi

[1]Department of Mathematics RSKD PG College, U.P., India.

[2]Department of Mathematics RSKD PG College, U.P., India.

[3]Department of Applied Sciences, Jahangirabad Institute of Technology, U.P., India

Abstract : In this paper, we have emphasized for study of Soret-Dufour effect and radiation absorption on unsteady MHD Casson fluid flow past a vertical plate embedded in porous medium in the existence of radiation and heat generation/absorption. Non-dimensional governing equations of flow filed for this study have been solved numerically using the Crank-Nicolson implicit finite difference method. With the help of graphs and tables, the effect of non-dimensional parameters on Concentration, temperature and velocity profiles are studied. Others parameter like skin friction, Nusselt number and Sherwood number at dependency of various parameters are inspected through tables.

IndexTerms **- Casson Fluid, Radiation absorption, Magnetohydrodynamics, Order of chemical reaction, Soret and Dufour effects.**

I. INTRODUCTION

It is a large number of applications of Non-Newtonian fluid flow filed in the presence of several effects so that many mathematicians have attained their great attention. Casson fluid is one of type of non-Newtonian fluid which reveals elasticity in nature, some examples of Casson fluid are jelly, honey, tomato sauce. Human blood can also be treated as Casson fluid. Liaquat Ali Lund et al.[1] is investigated the magnetohydrodynamic (MHD) flow of Casson nanofluid with thermal radiation over an unsteady shrinking surface. Shahanaz Parvin et al.[2] are discussed effects of the mixed convection parameter, concentration buoyancy ratio parameter, Soret–Dufour parameters, and shrinking parameter in MHD Casson fluid flow past shrinking sheet. Lahmar et al.[3] studied heat transfer of squeezing unsteady nanofluid flow under the effects of an inclined magnetic field and variable thermal conductivity. Mohamed R.Eid et al. [4] investigated numerically for Carreau nanofluid flow over a convectively heated nonlinear stretching surface with chemically reactive species. Hammad Alotaibi et al.[5] introduced the effect of heat absorption (generation) and suction (injection) on magnetohydrodynamic (MHD) boundary-layer flow of Casson nanofluid (CNF) via a non-linear stretching surface with the viscous dissipation in two dimensions. Asogwa and Ibe [6] investigated numerical approach of MHD Casson fluid flow over a permeable stretching sheet with heat and mass transfer taking into cognizance the various parameters present. Renu et al.[7] assessed the effect of the inclined outer velocity on heat and flow transportation in boundary layer Casson fluid over a stretching sheet. Ramudu et al. [8] highlighted the impact of magnetohydrodynamic Casson fluid flow across a convective surface with cross diffusion, chemical reaction, non-linear radiative heat. Recently Mahabaleshwar et al.[9] discussed the important roles of SWCNTs and MWCNTs under the effect of magnetohydrodynamics nanofluids flow past over the stretching/shrinking sheet under the repercussions of thermal radiation and Newtonian heating. In this investigation our aim is to bring to light the effect of unsteady MHD Casson fluid flow through a vertical porous plate with Soret-Dufour, radiation absorption, heat source/sink and higher-order chemical reaction. The influence of various physical parameters on velocity, temperature and concentration profiles is discussed with the help of tables and graphs. On the other hand important physical quantities like shearing stress, Nusselt number and Sherwood number are discussed through tables.

II. Mathematical Model

The unsteady MHD flow of a viscous incompressible electrically conducting Casson fluid past an impulsively started infinite inclined porous plate with variable temperature and mass diffusion in the presence of radiation has been considered. The plate is vertical and is embedded in porous medium. The x- axis is taken along the plate and y-axis is taken normal to it. Initially, It is also assumed that the radiation heat flux in x- direction is negligible as compared to that in y -direction. The plate and fluid are at the same temperature and concentration. At time t, the plate is given impulsive motion along x-direction against gravitational field with constant velocity u_0 , the plate temperature and concentration decrease exponentially with time. The transversely applied

magnetic field and magnetic Reynolds number are very small and hence induced magnetic field is negligible, Cowling [11]. Due to infinite length in x-direction, the flow variables are functions of y and t only. Under the usual Boussinesq's approximation, governing equations for this unsteady problem are given by:

Continuity equation:

$$\frac{\partial \bar{v}}{\partial \bar{y}} = 0 \quad \Rightarrow \ \bar{v} = -v_0 (constant) \tag{1}$$

Momentum equation:

$$\frac{\partial \bar{u}}{\partial \bar{t}} + \bar{v}\frac{\partial \bar{u}}{\partial \bar{y}} = \nu\left(1+\frac{1}{\beta}\right)\frac{\partial^2 \bar{u}}{\partial \bar{y}^2} + g\,\beta_t(\bar{T}-\bar{T}_\infty) + g\,\beta_c(\bar{C}-\bar{C}_\infty) - \frac{\sigma {B_0}^2 \bar{u}}{\rho} - \frac{\mu \bar{u}}{\rho_\infty \bar{K}} \tag{2}$$

Energy equation:

$$\rho_\infty C_p\left(\frac{\partial \bar{T}}{\partial \bar{t}} + \bar{v}\frac{\partial \bar{T}}{\partial \bar{y}}\right) = k\frac{\partial^2 \bar{T}}{\partial \bar{y}^2} - \frac{\partial q_r}{\partial \bar{y}} + \frac{\rho D_m K_T}{c_s}\frac{\partial^2 \bar{C}}{\partial \bar{y}^2} - \bar{Q}_0\left(\bar{T}-\bar{T}_\infty\right) + Q_1\left(\bar{C}-\bar{C}_\infty\right) \tag{3}$$

$$\frac{\partial \bar{C}}{\partial \bar{t}} + \bar{v}\frac{\partial \bar{C}}{\partial \bar{y}} = D\frac{\partial^2 \bar{C}}{\partial \bar{y}^2} + \frac{D_m K_T}{T_m}\frac{\partial^2 \bar{T}}{\partial \bar{y}^2} - k_r\left(\bar{C}-\bar{C}_\infty\right)^n \tag{4}$$

$k_r\left(\bar{C}-\bar{C}_\infty\right)^n$	terms in mass equation for higher order chemical reaction
n	order of chemical reaction
k_r	chemical reaction constant
$\bar{C}$	concentration
$\bar{T}$	temperature
$\bar{T}_\infty$	temperature of free stream
$\bar{C}_\infty$	concentration of free stream
β	Casson parameter
βc	coefficient of volume expansion for mass transfer
β_t	volumetric coefficient of thermal expansion
T_m	mean fluid temperature
q_r	radiative heat along y ∗ -axis
$\bar{Q}_0$	Coefficient of heat source/sink
$\bar{Q}_1$	Radiation absorption parameter
ν	kinematic viscosity
$\bar{K}$	coefficient of permeability of porous medium
D_m	molecular diffusivity
k	thermal conductivity of fluid
c_p	specific heat at constant pressure
μ	viscosity
ρ	fluid density
σ	electrical conductivity
g	acceleration due to gravity
K_T	thermal diffusion ratio

In equation 4; $k_r\left(\bar{C}-\bar{C}_\infty\right)^n$ has come on account of nth order chemical reaction.

The boundary conditions for this model are assumed as:

$$\left.\begin{array}{llll} \bar{t} \le 0; & \bar{u} = 0, \quad v_0 = -v_0 & \overline{T} = \overline{T}_\infty, \quad \overline{C} = \overline{C}_\infty & \forall\, \bar{y} \\ \bar{t} > 0; & \bar{u} = u_0, \ \overline{T} = \overline{T}_\infty + (\overline{T}_w - \overline{T}_\infty)e^{-At}, \ \overline{C} = \overline{C}_\infty + (\overline{C}_w - \overline{C}_\infty)e^{-At} & at\ \bar{y} = 0 \\ & \bar{u} \to 0, \quad \overline{T} \to \overline{T}_\infty, \quad \overline{C} \to \overline{C}_\infty & as\ \ \bar{y} \to \infty \end{array}\right\} \quad (5)$$

Where $A = \dfrac{V_0^{\,2}}{\nu}$

Roseland explained the term radiative heat flux approximately as

$$q_r = -\frac{4\sigma_{st}}{3a_m}\frac{\partial \overline{T}^{\,4}}{\partial\, \bar{y}^4} \quad (6)$$

Here Stefan Boltzmann constant and absorption coefficient are σ_{st} and a_m respectively.

In this case temperature differences are very-very small within flow, such that $\overline{T}^{\,4}$ can be expressed linearly with temperature. It is realized by expanding in a Taylor series about T_∞' and neglecting higher order terms, so

$$\overline{T}^{\,4} \sim= 4\overline{T}_\infty^{\,3}\overline{T} - 3\overline{T}_\infty^{\,4} \quad (7)$$

With the help of equations (6) and (7), we write the equation (3) in this way

$$\rho_\infty C_p\left(\frac{\partial \overline{T}}{\partial \bar{t}} + \bar{v}\frac{\partial \overline{T}}{\partial \bar{y}}\right) = k\frac{\partial^2 \overline{T}}{\partial\, \bar{y}^2} + \frac{16\overline{T}_\infty^{\,3}\sigma_{st}}{3a_m}\frac{\partial^2 \overline{T}}{\partial\, \bar{y}^2} + \frac{\rho D_m K_T}{c_s}\frac{\partial^2 \overline{C}}{\partial\, \bar{y}^2} - \overline{Q}_0\left(\overline{T} - \overline{T}_\infty\right) + Q_1\left(\overline{C} - \overline{C}_\infty\right) \quad (8)$$

Let us introduce the following dimensionless quantities

$$\left.\begin{array}{l} u = \dfrac{\bar{u}}{u_0}, t = \dfrac{\bar{t}v_0^{\,2}}{\nu}, y = \dfrac{\bar{y}v_0}{\nu}, \theta = \dfrac{\overline{T} - \overline{T}_\infty}{\overline{T}_w - \overline{T}_\infty}, C = \dfrac{\overline{C} - \overline{C}_\infty}{\overline{C}_w - \overline{C}_\infty}, \\ G_m = \dfrac{\nu g\beta_c(\overline{C}_w - \overline{C}_\infty)}{u_0 v_0^{\,2}}, G_r = \dfrac{\nu\, g\beta(\overline{T}_w - \overline{T}_\infty)}{u_0 v_0^{\,2}}, K = \dfrac{v_0^{\,2}}{\nu^2}\overline{K}, \\ S_c = \dfrac{\nu}{D}, P_r = \dfrac{\mu C_p}{k}, M = \dfrac{\sigma B_0^{\,2}\nu}{\rho v_0^{\,2}}, R = \dfrac{4\sigma \overline{T}_\infty^{\,3}}{k_m k}, \\ K_r = \dfrac{k_r \nu}{v_0^{\,2}}, A = \dfrac{v_0^{\,2}}{\nu}, Q = \dfrac{Q_0\nu}{\rho c_p v_0^{\,2}}, D_u = \dfrac{D_m K_T(\overline{C}_w - \overline{C}_\infty)}{c_s c_p \nu(\overline{T}_w - \overline{T}_\infty)}, \\ \overline{Q} \\ S_r = \dfrac{D_m K_T(\overline{T}_w - \overline{T}_\infty)}{T_m \nu(\overline{C}_w - \overline{C}_\infty)}, Q_c = \dfrac{Q_1\nu(\overline{C} - \overline{C}_\infty)}{\rho c_p v_0^{\,2}(\overline{T}_w - \overline{T}_\infty)} \end{array}\right\} \quad (9)$$

Using substitutions of Equation 9, we get non-dimensional form of partial differential Equations 2, 8 and 4 respectively:

$$\frac{\partial u}{\partial t} - \frac{\partial u}{\partial y} = \left(1 + \frac{1}{\beta}\right)\frac{\partial^2 u}{\partial y^2} + G_r\theta + G_m C - \left(M + \frac{1}{K}\right)u \quad (10)$$

$$\frac{\partial \theta}{\partial t} - \frac{\partial \theta}{\partial y} = \frac{1}{P_r}\left(1 + \frac{4R}{3}\right)\frac{\partial^2 \theta}{\partial y^2} + D_u\frac{\partial^2 C}{\partial y^2} - Q\theta - Q_c C \quad (11)$$

$$\frac{\partial C}{\partial t}-\frac{\partial C}{\partial y}=\frac{1}{S_c}\frac{\partial^2 C}{\partial y^2}+S_r\frac{\partial^2\theta}{\partial y^2}-K_rC^n \tag{12}$$

with initial and boundary conditions

$$\left.\begin{array}{llll} t\le 0; & u=0, \quad \theta=0, & C=0 & \forall y \\ t>0; & u=1, \quad \theta=e^{-t}, & C=e^{-t} & at\ y=0 \\ u\to 0, & \theta\to 0, & C\to 0 & as\ y\to\infty \end{array}\right\} \tag{13}$$

The degree of practical attention include the Skin friction coefficients Cf , local Nusselt Nu, and local Sherwood Sh numbers are known as follows:

$$C_f=-\left(1+\frac{1}{\beta}\right)\left(\frac{\partial u}{\partial y}\right)_{y=0},\ N_u=-\left(\frac{\partial\theta}{\partial y}\right)_{y=0},\ Sh=-\left(\frac{\partial C}{\partial y}\right)_{y=0} \tag{14}$$

III. Numerical Method of Solution

Exact solution of system of partial differential equations 10, 11 and 12 with boundary conditions 13 are impossible. So, these are solved using Crank-Nicolson implicit finite difference method. The Crank-Nicolson implicit finite difference method is a second order method in time ($o(\Delta t^2)$) and has no restriction on space and time steps, that is, the method is unconditionally stable. The computation is executed for $\Delta y = 0.1$, $\Delta t = 0.001$ and procedure is repeated till $y = 4$. Equations 10, 11 and 12 are expressed as

$$\frac{u_{i,j+1}-u_{i,j}}{\Delta t}-\frac{u_{i+1,j}-u_{i,j}}{\Delta y}=\left(1+\frac{1}{\beta}\right)\frac{u_{i-1,j}-2u_{i,j}+u_{i+1,j}+u_{i-1,j+1}-2u_{i,j+1}+u_{i+1,j+1}}{2(\Delta y)^2}$$
$$+G_r\left(\frac{\theta_{i,j+1}+\theta_{i,j}}{2}\right)+G_m\left(\frac{C_{i,j+1}+C_{i,j}}{2}\right)-M\left(1+\frac{1}{K}\right)\left(\frac{u_{i,j+1}+u_{i,j}}{2}\right) \tag{15}$$

$$\frac{\theta_{i,j+1}-\theta_{i,j}}{\Delta t}-\frac{\theta_{i+1,j}-\theta_{i,j}}{\Delta y}=\frac{1}{P_r}\left(1+\frac{4R}{3}\right)\left(\frac{\theta_{i-1,j}-2\theta_{i,j}+\theta_{i+1,j}+\theta_{i-1,j+1}-2\theta_{i,j+1}+\theta_{i+1,j+1}}{2(\Delta y)^2}\right)$$
$$+D_u\left(\frac{C_{i-1,j}-2C_{i,j}+C_{i+1,j}+C_{i-1,j+1}-2C_{i,j+1}+C_{i+1,j+1}}{2(\Delta y)^2}\right)-Q\left(\frac{\theta_{i,j+1}+\theta_{i,j}}{2}\right)$$
$$-Q_c\left(\frac{C_{i,j+1}+C_{i,j}}{2}\right) \tag{16}$$

$$\frac{C_{i,j+1}-C_{i,j}}{\Delta t}-\frac{C_{i+1,j}-C_{i,j}}{\Delta y}=\frac{1}{S_C}\left(\frac{C_{i-1,j}-2C_{i,j}+C_{i+1,j}+C_{i-1,j+1}-2C_{i,j+1}+C_{i+1,j+1}}{2(\Delta y)^2}\right)$$
$$+S_r\left(\frac{\theta_{i-1,j}-2\theta_{i,j}+\theta_{i+1,j}+\theta_{i-1,j+1}-2\theta_{i,j+1}+\theta_{i+1,j+1}}{2(\Delta y)^2}\right)+K_r\left(\frac{C_{i,j+1}+C_{i,j}}{2}\right)^n \tag{17}$$

Initial and boundary conditions are also rewritten as:

$$\left.\begin{array}{llll} u_{i,0}=0, & \theta_{i,0}=0, & C_{i,0}=0 & \forall i \\ u_{0,j}=1, & \theta_{0,j}=e^{-j\Delta t}, & C_{0,j}=e^{-j\Delta t} & \forall j \\ u_{n,j}\to 0, & \theta_{n,j}\to 0, & C_{n,j}\to 0 & \end{array}\right. \tag{18}$$

Where index i represents to y and j represents to time t, $\Delta t = tj+1-tj$ and $\Delta y = yi+1-yi$. Getting the values of u, θ and C at time t, we may compute the values at time $t+\Delta t$ as following method: we substitute i = 1, 2, ..., n−1 , where n correspond to ∞ ,equations 15 to 17 give tridiagonal system of equations with boundary conditions in equation 18, are solved employing Thomas algorithm

as discussed in Carnahan et al.[10], we find values of θ and C for all values of y at t + Δt. Equation 15 is solved by same to substitute these values of θ and C, we get solution for u till desired time t.

IV. Analysis of Result

The present work analyzes the boundary layer unsteady MHD Casson flow past a porous vertical plate with the Soret-Dufour effect. The influence of the order of chemical reaction has been incorporated in the mass equation. In order to see a physical view of work, numerical results of velocity profile u, temperature profile θ, concentration profile C have been discussed with the help of graphs and skin friction coefficients, Nusselt number and Sherwood number are discussed with the help of tables. The following values are used for investigation Gr = 3, Gm = 6 and K = 1.2. The effect of magnetic parameter M on velocity u is depicted in figure 20. It has seen that fluid velocity decreasing with an increase in M. It is noted from figure 17 that increasing radiation parameter R, velocity u increases. This is correct observation because the increase in radiation reveals heat energy to flow. In figure 19, velocity decreases as Prandtl number Pr increases and temperature decreases in figure 13 when Pr increases. In figure 2 concentration C near to plate decreases and some distance from plate concentration increases as Prandtl number increases. Figure 10 depicts the importance of radiation on temperature distribution. It is analyzed that an increase in R, temperature θ increases and it is notable that an increase in R concentration C near to plate decrease after that increases in figure 7. Figure 6 depicts the variation of Schmidt number Sc as concentration decreases rapidly with increase Sc. It is noteworthy that on increasing Schmidt numbers Sc temperature profile in figure 9 increases near to plate only while velocity profile in figure 16 decreases near to plate. We demonstrate the influence of Soret number in velocity, temperature and concentration in figure 24, 15 and 5 respectively. It is analyzed that an increase in Sr, velocity u increases; temperature decreases near to plate after then increase and concentration increases rapidly. In figure 22, 4 and 14, it is seen that velocity increases and concentration decreases as increase Dufour number Du, whereas temperature increases as Du increases. Figures 21 and 3 depict the behavior of chemical reaction parameter Kr on velocity and concentration respectively. It is seen that velocity decreases; temperature increases slowly as Kr increases and concentration decreases rapidly as Kr increase. The negative value of $Q < 0$ means heat absorption and the positive value of $Q > 0$ means heat transfer. In figure 18, velocity profile decreases on increasing heat source/sink parameter Q and also reducing momentum boundary layer. Figure 12 analyzed the impact of heat source/sink parameter Q in the temperature profile. It can be seen that the temperature profile decreases rapidly and the thermal boundary layer reduces for an increase of heat source parameter but it increases with the heat sink parameter. Figure 1, depicts that concentration profile increases near to plate from middle of boundary layer it decreases as well as species boundary layer reduces on an increase of heat source/sink parameter. The influence of Radiation absorption parameter Q_c on the concentration and temperature profiles in figure 8 and figure 11 have been shown. We observe that when an increase Q_c results in the concentration profile also decreases while temperature increases. Figure 23, shows the effect of Casson fluid parameter β on velocity profile. It is observed that velocity increase near to plate increases after then decreases as well as momentum boundary layer reduces on increasing Casson fluid parameter.

It is observed from **Table 1** that M increases, the skin friction coefficient increases. Change in Schmidt number Sc, Pr and Pr effects as skin friction coefficient and Sherwood number increases while Nusselt number decreases. Skin friction coefficient and Sherwood number decrease whereas Nusselt number increases when Dufour number Du and radiation parameter R increase. Increase in Soret number Sr, and Nusselt number Nu and Sherwood number increase while Skin friction decreases. On increasing Casson fluid parameter β results in skin friction decreases. It is also noted that increment in Q heat source/sink the skin friction coefficient and Sherwood number increases while Nusselt number decreases. Skin friction coefficient and Sherwood number decrease whereas Nusselt number increases when Qc heat absorption parameter increase.

V. Conclusion

Effect of second-order chemical reaction, change in Soret-Dufour on unsteady MHD flow past a vertical porous plate immersed in a porous medium are analyzed. This investigation the following conclusions have come:

1. The effect of radiation on concentration is noteworthy. It is observed that increasing values of R, concentration falls down and after some distance from the plate, it goes up slowly-slowly. Interestingly, the same type of change in concentration has been found on increasing Prandtl number P r.
2. For increasing values of Kr, it is a considerable enhancement in velocity, i.e. velocity decreases slowly.
3. Increasing values of Soret and Dufour number, it is observed that temperature profile in the thermal boundary layer increases whereas temperature profile first decreases after then increases slowly in the boundary layer.
4. Schmidt number greatly influences the concentration profile in the concentration boundary layer.

Conflicts of Interest

The authors declare that there is no conflict of interest regarding the publication of this paper.

Acknowledgements

We acknowledge our principal Prof. Shambhu Ram and Prof Akhieleshwar Shukla and thank for encourage to complete this research work.

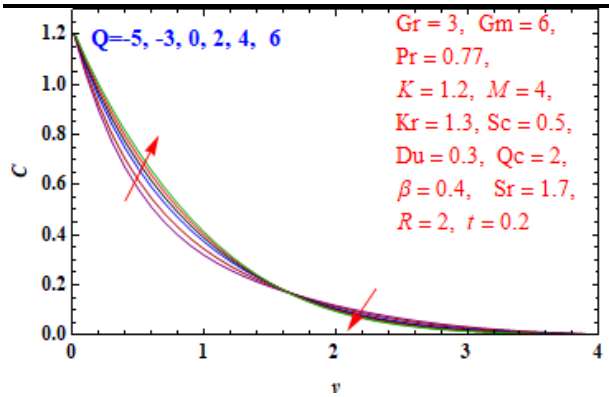

Fig. 1 Concentration Profiles for Different Values of Q

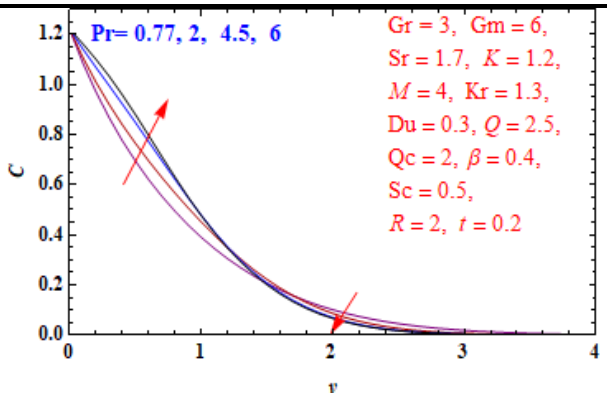

Fig. 2 Concentration Profiles for Different Values of Pr

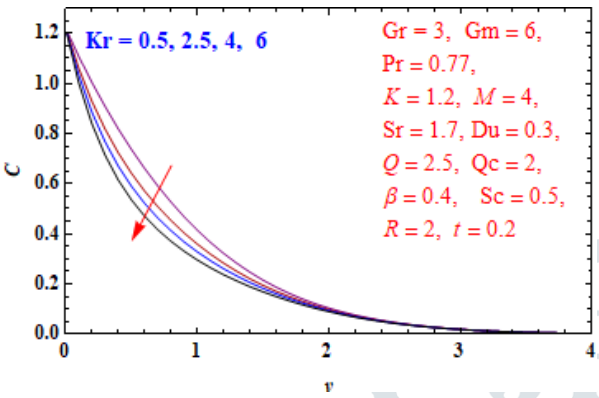

Fig. 3 Concentration Profiles for Different Values of Kr

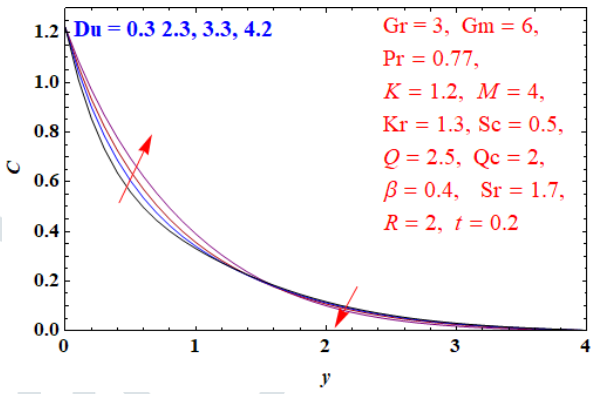

Fig. 4 Concentration Profiles for Different Values of Du

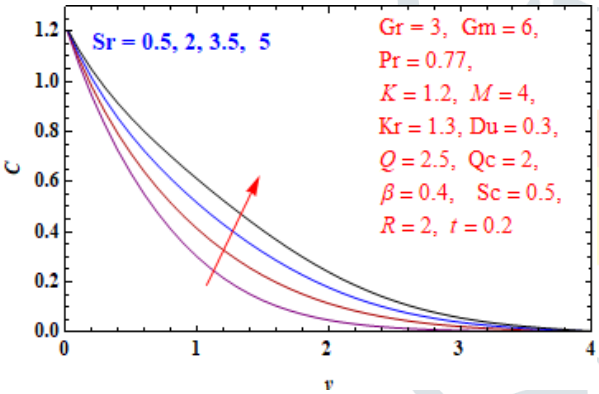

Fig. 5 Concentration Profiles for Different Values of Sr

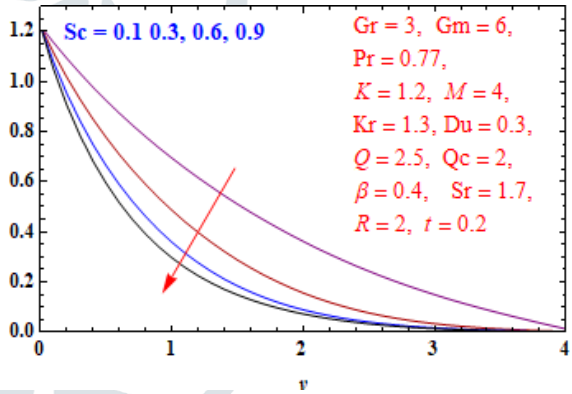

Fig. 6 Concentration Profiles for Different Values of Sc

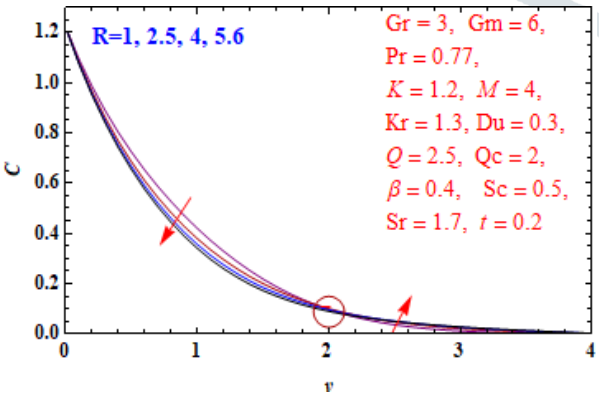

Fig. 7 Concentration Profiles for Different Values of R

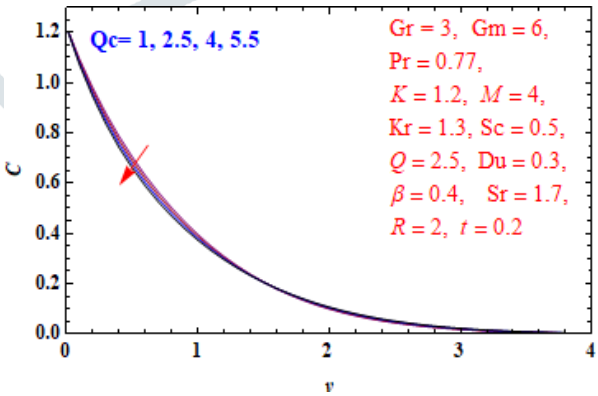

Fig. 8 Concentration Profiles for Different Values of Qc

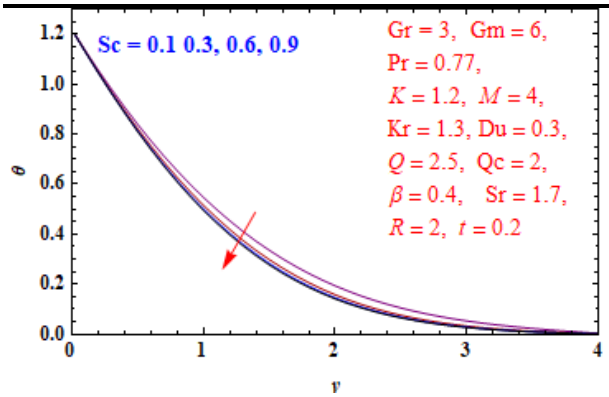

Fig. 9 Temperature Profiles for Different Values of Sc

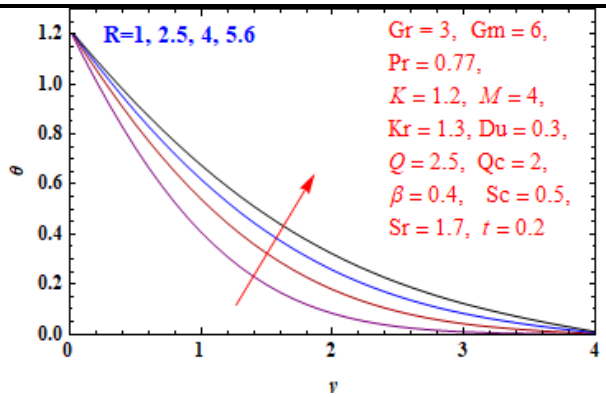

Fig. 10 Temperature Profiles for Different Values of R

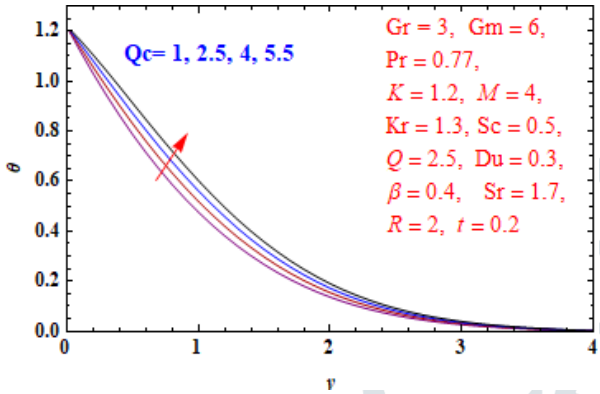

Fig. 11 Temperature Profiles for Different Values of Qc

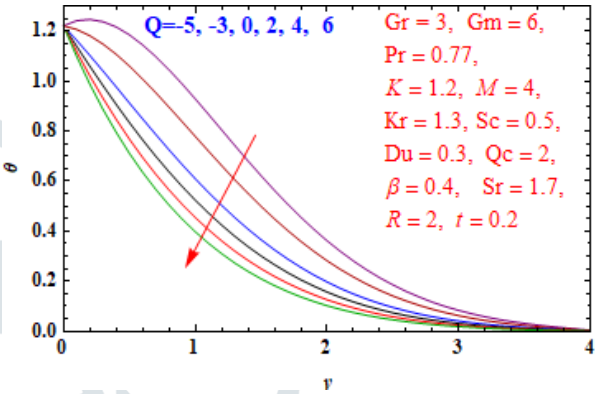

Fig. 12 Temperature Profiles for Different Values of Q

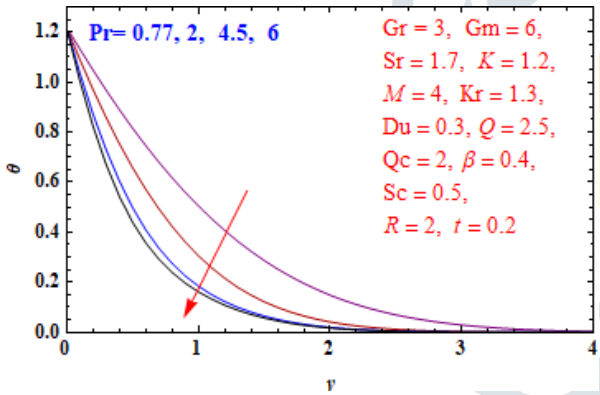

Fig. 13 Temperature Profiles for Different Values of Pr

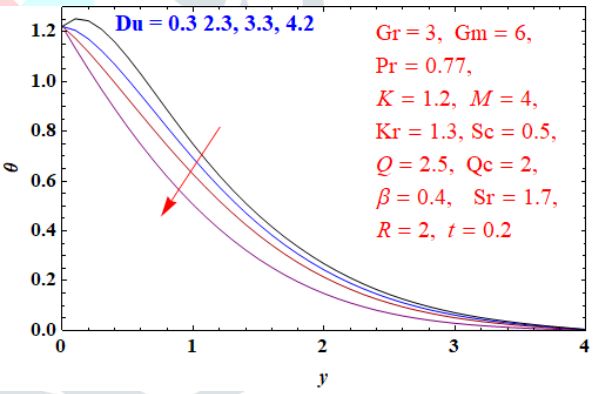

Fig. 14 Temperature Profiles for Different Values of Du

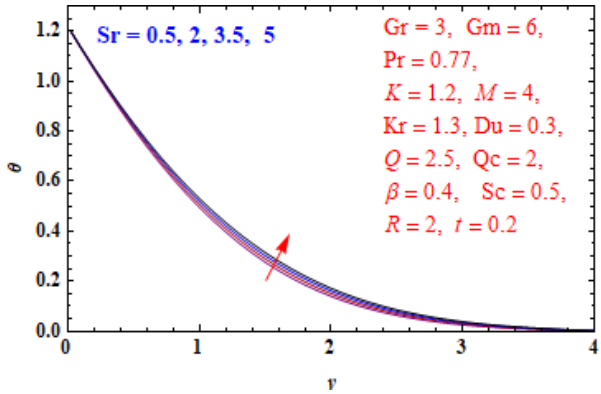

Fig. 15 Temperature Profiles for Different Values of Sr

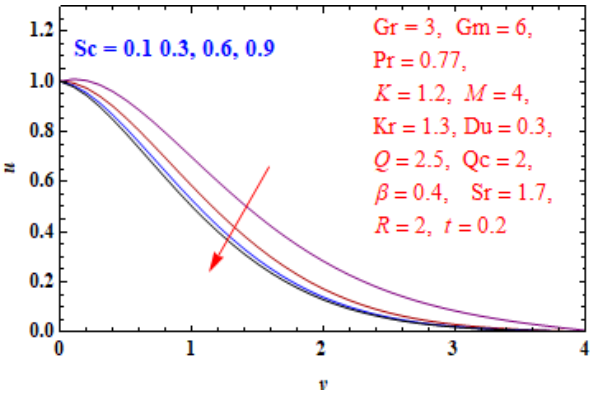

Fig. 16 Temperature Profiles for Different Values of Sc

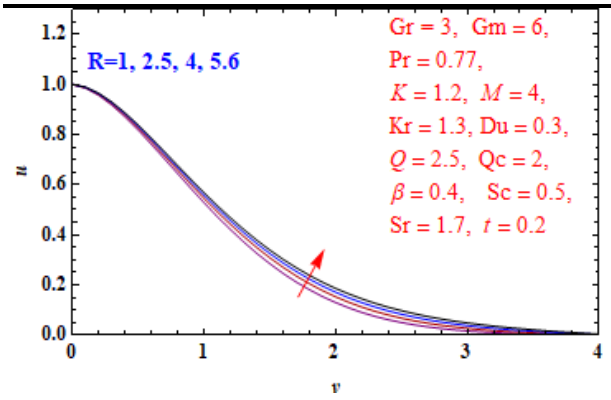

Fig. 17 Velocity Profiles for Different Values of R

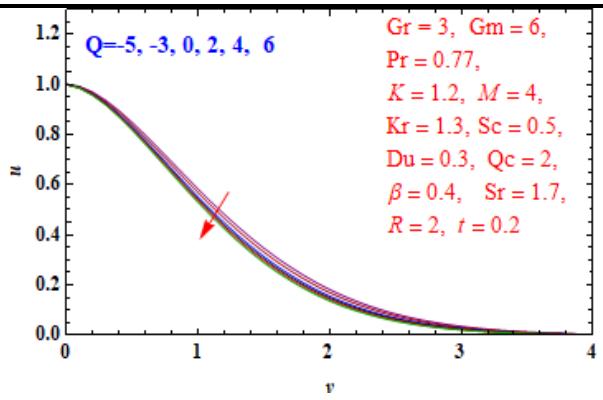

Fig. 18 Velocity Profiles for Different Values of Q

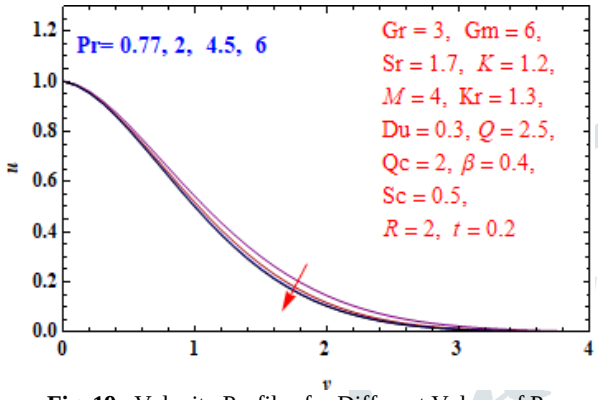

Fig. 19 Velocity Profiles for Different Values of Pr

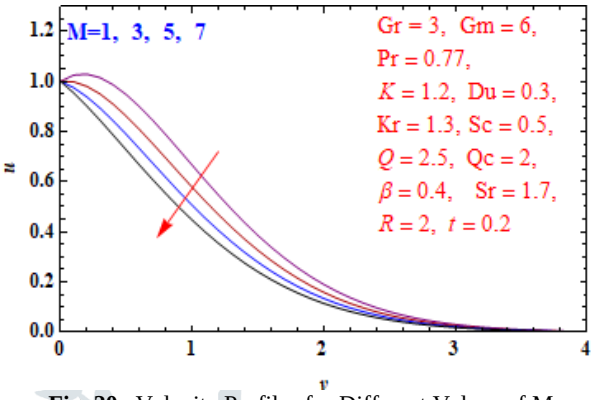

Fig. 20 Velocity Profiles for Different Values of M

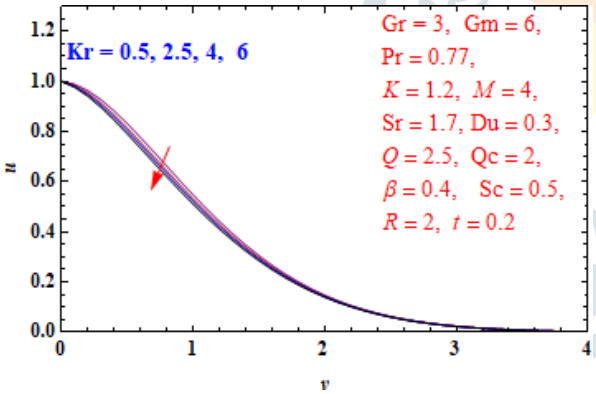

Fig. 21 Velocity Profiles for Different Values of Kr

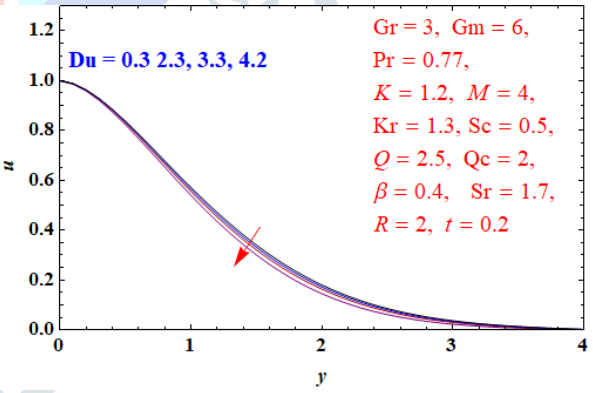

Fig. 22 Velocity Profiles for Different Values of Du

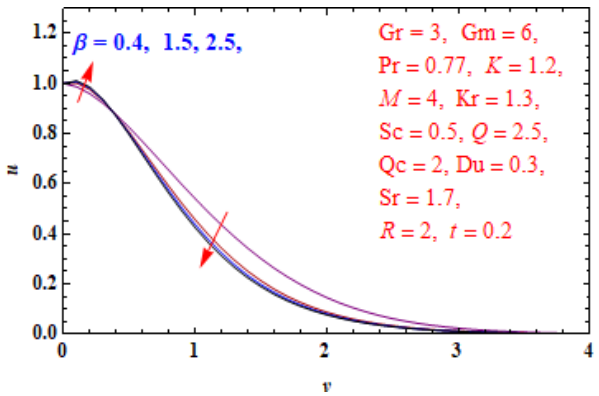

Fig. 23 Velocity Profiles for Different Values of β

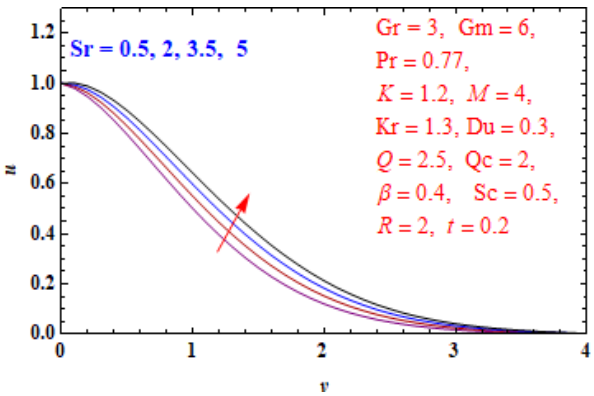

Fig. 24 Velocity Profiles for Different Values of Sr

Table 1. Skin friction coefficient τ, Nusselt number Nu and Sherwood number Sh for different values of parameters taking fix values of Gr = 3, Gm = 6, K = 1.2

β	Du	Kr	M	Pr	Q	Q_c	R	S_c	S_r	τ	Nu	Sh
0.4	0.3	1.3	4	0.77	2.5	2	2	0.5	1.7	0.482756	0.872999	1.3385
1.5	0.3	1.3	4	0.77	2.5	2	2	0.5	1.7	-0.0245151	0.872999	1.3385
2.5	0.3	1.3	4	0.77	2.5	2	2	0.5	1.7	-0.0901581	0.872999	1.3385
4	0.3	1.3	4	0.77	2.5	2	2	0.5	1.7	-0.124611	0.872999	1.3385
0.4	**0.3**	1.3	4	0.77	2.5	2	2	0.5	1.7	0.482756	0.872999	1.3385
0.4	**2.3**	1.3	4	0.77	2.5	2	2	0.5	1.7	0.437418	0.47406	1.56847
0.4	**3.3**	1.3	4	0.77	2.5	2	2	0.5	1.7	-0.119433	0.154873	1.76991
0.4	**4.2**	1.3	4	0.77	2.5	2	2	0.5	1.7	-0.116142	-0.311515	2.08668
0.4	0.3	**0.5**	4	0.77	2.5	2	2	0.5	1.7	0.400182	0.876834	1.13117
0.4	0.3	**2.5**	4	0.77	2.5	2	2	0.5	1.7	0.588875	0.867891	1.60421
0.4	0.3	**4**	4	0.77	2.5	2	2	0.5	1.7	0.699089	0.862297	1.88079
0.4	0.3	**6**	4	0.77	2.5	2	2	0.5	1.7	0.818496	0.855793	2.18331
0.4	0.3	1.3	**1**	0.77	2.5	2	2	0.5	1.7	-0.884802	0.872999	1.3385
0.4	0.3	1.3	**3**	0.77	2.5	2	2	0.5	1.7	0.0561309	0.872999	1.3385
0.4	0.3	1.3	**5**	0.77	2.5	2	2	0.5	1.7	0.884033	0.872999	1.3385
0.4	0.3	1.3	**7**	0.77	2.5	2	2	0.5	1.7	1.62014	0.872999	1.3385
0.4	0.3	1.3	4	**0.77**	2.5	2	2	0.5	1.7	0.482756	0.872999	1.3385
0.4	0.3	1.3	4	**2**	2.5	2	2	0.5	1.7	0.559488	1.28533	1.12779
0.4	0.3	1.3	4	**4.5**	2.5	2	2	0.5	1.7	0.587986	1.83118	0.788015
0.4	0.3	1.3	4	**6**	2.5	2	2	0.5	1.7	0.588863	2.12142	0.587507
0.4	0.3	1.3	4	0.77	**-5**	2	2	0.5	1.7	0.309589	-0.205951	1.178989
0.4	0.3	1.3	4	0.77	**-3**	2	2	0.5	1.7	0.370301	0.143669	1.65478
0.4	0.3	1.3	4	0.77	**0**	2	2	0.5	1.7	0.439665	0.575789	1.47357
0.4	0.3	1.3	4	0.77	**2**	2	2	0.5	1.7	0.47501	0.817311	1.36451
0.4	0.3	1.3	4	0.77	**4**	2	2	0.5	1.7	0.503758	1.03034	1.26324
0.4	0.3	1.3	4	0.77	**6**	2	2	0.5	1.7	0.527266	1.22038	1.1687
0.4	0.3	1.3	4	0.77	2.5	**1**	2	0.5	1.7	0.494434	0.969237	1.29139
0.4	0.3	1.3	4	0.77	2.5	**2.5**	2	0.5	1.7	0.476985	0.825476	1.36183
0.4	0.3	1.3	4	0.77	2.5	**4**	2	0.5	1.7	0.459934	0.685249	1.43092
0.4	0.3	1.3	4	0.77	2.5	**5.5**	2	0.5	1.7	0.443273	0.548451	1.4987
0.4	0.3	1.3	4	0.77	2.5	2	**1**	0.5	1.7	0.524466	1.04797	1.25503
0.4	0.3	1.3	4	0.77	2.5	2	**2.5**	0.5	1.7	0.465159	0.815659	1.36369
0.4	0.3	1.3	4	0.77	2.5	2	**4**	0.5	1.7	0.421478	0.697961	1.41169
0.4	0.3	1.3	4	0.77	2.5	2	**5**	0.5	1.7	0.385303	0.618644	1.4411
0.4	0.3	1.3	4	0.77	2.5	2	2	**0.1**	1.7	-0.314314	0.831177	0.665427
0.4	0.3	1.3	4	0.77	2.5	2	2	**0.3**	1.7	0.231936	0.863814	1.0751
0.4	0.3	1.3	4	0.77	2.5	2	2	**0.6**	1.7	0.569801	0.874937	1.44713
0.4	0.3	1.3	4	0.77	2.5	2	2	**0.9**	1.7	0.757069	0.876194	1.72234
0.4	0.3	1.3	4	0.77	2.5	2	2	0.5	**0.5**	-0.691683	0.884801	1.49364
0.4	0.3	1.3	4	0.77	2.5	2	2	0.5	**2**	0.431772	0.870138	1.30074
0.4	0.3	1.3	4	0.77	2.5	2	2	0.5	**3.5**	0.183893	0.856355	1.11749
0.4	0.3	1.3	4	0.77	2.5	2	2	0.5	**5**	-0.0529867	0.843401	0.942474

References

[1] Shafiq A., Rasool G. and Tlili I.(2020) Marangoni convective nanofluid flow over an electromagnetic actuator in the presence of first-order chemical reaction. Heat Transf. Asian Res, 49, 274–288.

[2] Parvin S.; Mohamed Isa S.S.P., Arifin, N.M., Md Ali, F.(2021) The Inclined Factors of Magnetic Field and Shrinking Sheet in Casson Fluid Flow, Heat and Mass Transfer. Symmetry, 13, 373. https://doi.org/10.3390/ sym13030373.

[3] Lahmar Sihem, Kezzar Mohamed, Eid Mohamed R., and Sari, Mohamed Rafik, (2020) Heat transfer of squeezing unsteady nanofluid flow under the effects of an inclined magnetic field and variable thermal conductivity, Physica A: Statistical Mechanics and its Applications, Elsevier, vol. 540(C).

[4] M. R. Eid, K. Mahny, A. Dar and T. Muhammad, (2020) Numerical study for Carreau nanofluid flow over aconvectively heated nonlinear stretching surface with chemically reactive species, Physica A: Statistical Mechanics and Its Applications, 540, 123063.

[5] Hammad Alotaibi, Saeed Althubiti, Mohamed R. Eid, K. L. Mahny, (2021) Numerical Treatment of MHD Flow of Casson Nanofluid via Convectively Heated Non-Linear Extending Surface with Viscous Dissipation and Suction/Injection Effects, 66(1), 229-245, doi:10.32604/cmc.2020.012234.

[6] K. K. Asogwa and A. A. Ibe, (2020) A Study of MHD Casson Fluid Flow over a Permeable Stretching Sheet with Heat and Mass Transfer, Journal of Engineering Research and Reports, 16(2), 10-25.

[7] Renu Devi, Vikas Poply, Manimala, (2021) Effect of aligned magnetic field and inclined outer velocity in casson fluid flow over a stretching sheet with heat source, Journal of Thermal Engineering, 7(4), 823-844.

[8] K Kumar Anantha, , Ankalagiri Ramudu Sugunamma Vangala, Dr.N. Sandeep, (2021) Impact of Soret and Dufour on MHD Casson fluid flow past a stretching surface with convective-diffusive conditions. Journal of Thermal Analysis and Calorimetry. 10.1007/s10973-021-10569-w.

[9] U. S. Mahabaleshwar, K. N. Sneha, Akio Miyara, M. Hatami (2022) Radiation effect on inclined MHD flow past a super-linear stretching/shrinking sheet including CNTs, Waves in Random and Complex Media, DOI: 10.1080/17455030.2022.2053238.

[10] Brice Carnahan, H.A. Luther and James O. Wilkes. (1990), Applied Numerical Methods, Krieger Pub Co, Florida.

[11] T. G. Cowling (1990), Magneto-Hydrodynamics, Inter Science Publishers, New York.